Heavy Quark Lifetimes, Mixing, and CP Violation

Guy Blaylock
Department of Physics and Astronomy
University of Massachusetts, Amherst, MA 01003

1 Introduction

Much has happened this year in the subject of heavy quark studies. This brief paper cannot hope to cover all of the details of work in this area, but will focus instead on a few of the highlights that have emerged. First of all, recent high precision measurements in charm lifetimes, particularly of the D_s, allow better understanding of the mechanism of charm decays. Secondly, a new search for charm mixing at CLEO significantly improves upon the sensitivity of previous analyses, and has implications for the effects of new physics in the charm sector. Thirdly, significant work has continued in the measurement of B_s mixing, which puts important constraints on the CKM parameter V_{td}. Finally, two of items of relevance to the study of CP violation in the B system have recently been made available, which will be touched on briefly.

2 Lifetimes

2.1 Charm lifetimes

To motivate the discussion of heavy quark lifetimes, it is useful to recall an old puzzle in charm physics. When researchers first measured the charged and neutral D meson lifetimes, they discovered that the D^+ lifetime was considerably longer (about a factor of 2.5) than the D^0 lifetime. This result ran counter to expectations. The decays of both mesons were believed to be dominated by the spectator decay of the charm quark (Figs. 1a and 1b), which suggested the two lifetimes should be nearly identical.

In the face of experimental evidence, several arguments were constructed as to why the two lifetimes might be different. First of all, the fact that there are two identical d quarks in the D^+ final state (and not in the D^0) might give rise to Pauli-type interference, which could extend the lifetime of the D^+. Moreover, other decay mechanisms, shown in Figs. 1c to 1f, were hypothesized, but these were expected to give only small contributions to the overall decay width. The D^+ could decay via the weak annihilation of the charm and anti-down quarks (Fig. 1c), but this

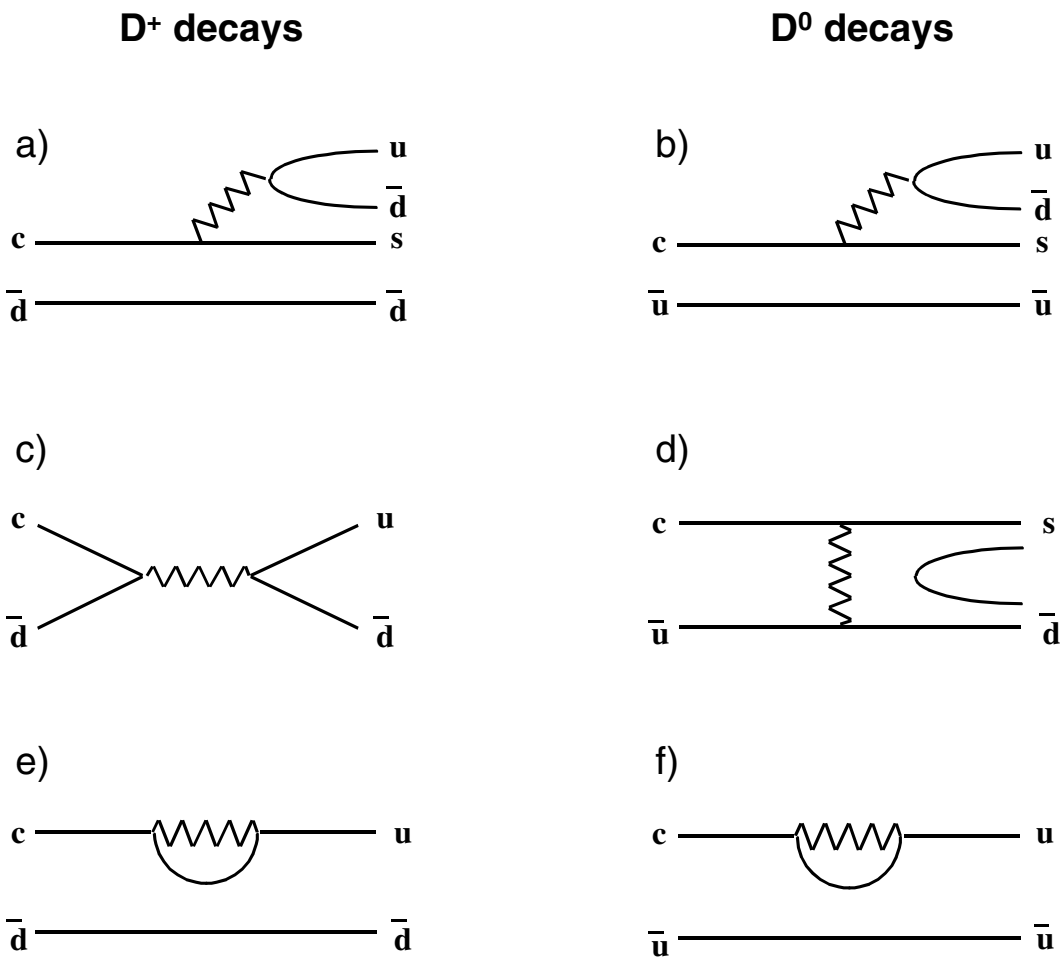

Figure 1: Diagrams contributing to D^+ and D^0 decay.

decay is Cabibbo suppressed, and therefore expected to be only a fraction of the spectator amplitude. Analogously, the D^0 could decay via the W exchange diagram of Fig. 1d, providing another difference between the two meson lifetimes. Both the weak annihilation and the W exchange amplitudes were expected to be small due to helicity and color suppression [1]. However, both forms of suppression could be circumvented by the emission of a soft gluon, so the strength of the suppression was in question. Finally, penguin diagrams such as Figs. 1e and 1f could also contribute, but these diagrams are Cabibbo, helicity, and color suppressed, and therefore received little attention.

In any case, the suggestion that mechanisms other than spectator quark decay could contribute significantly to the widths of the charm mesons provided motivation for further research in charm lifetimes. Primarily, this effort focused on lifetime

measurements of other weakly decaying charmed particles to use as comparisons. Interference patterns were expected to be different for charm baryons, thereby providing a handle on the effects of Pauli type interference. This is especially easy to see in the case of the Ω_c, where there are two identical strange quarks in the initial state. Moreover, W exchange is different for baryons, where the three quarks in the final state guarantee that the decay is neither helicity nor color suppressed. Finally, weak annihilation of charm and anti-strange quarks in D_s decay is not Cabibbo suppressed, offering the possibility of studying this contribution.

Figure 2 shows where we stand today in the measurement of charm lifetimes. All seven weakly decaying charmed particles are shown. The unlabeled error bars give the world averages from the 1998 PDG review [2]. Since then, new measurements have been made available on D^0 and D_s lifetimes from E791 [3], on all the D mesons from CLEO [4], and preliminary results on D_s and Λ_c from FOCUS and SELEX [5]. The most notable feature of the plot is that the D_s and D^0 lifetimes are measurably different. One year ago, these two lifetimes were nearly the same within errors. The new measurements not only reduce the error on the D_s lifetime, but also shift the central value. An average of currently available data, including preliminary results from FOCUS yields [5] $\tau_{D_s}/\tau_{D^0} = 1.211 \pm 0.017$.

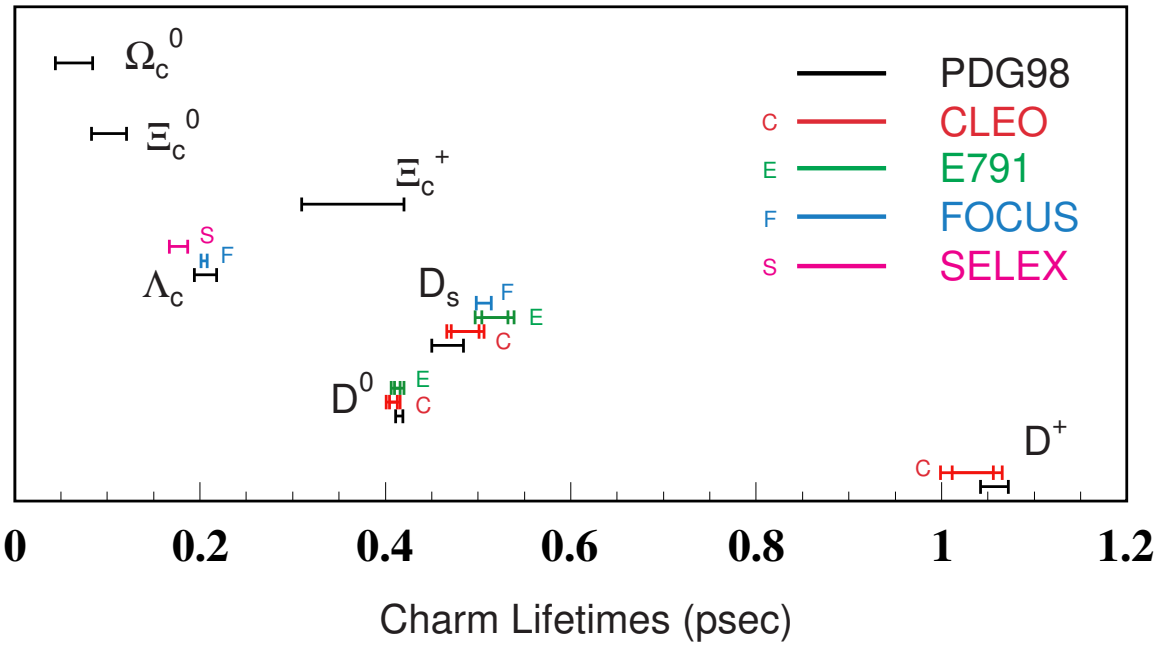

Figure 2: Measured lifetimes for all seven weakly decaying charmed particles.

The precision of these new lifetime measurements, and the promise of more to come from the Fermilab fixed target experiments, finally allows us to study charm

decays in a manner we have been wanting to do for 20 years [6]. As a simple example of how these data can be used to unravel the contributions to charm particle decay, consider the following three-step exercise to estimating Pauli interference, W exchange and weak annihilation contributions to D meson decays.

First of all, compare the doubly-Cabibbo suppressed decay $D^+ \to K^+\pi^+\pi^-$ to its Cabibbo favored counterpart $D^+ \to K^-\pi^+\pi^+$. Because the kinematics are nearly the same in the two cases, the decays differ in only two respects. First of all, the decay diagrams have different (well-known) weak couplings. Secondly, the Cabibbo-favored decay is subject to Pauli interference, while the DCS decay is not, because there are no identical particles in the DCS final state. The ratio of the two rates can therefore be expressed:

$$\frac{BR(D^+ \to K^+\pi^+\pi^-)}{BR(D^+ \to K^-\pi^+\pi^+)} \approx \frac{\Gamma_{SP}}{\Gamma_{PI}} \times \tan^4\theta_C, \tag{1}$$

where Γ_{PI} represents a spectator decay rate for the charm quark that is subject to Pauli interference, while Γ_{SP} represents a spectator decay rate without interference. A combination of current measurements, including preliminary FOCUS data, yields [5] $BR(D^+ \to K^+\pi^+\pi^-)/BR(D^+ \to K^-\pi^+\pi^+) = 0.68 \pm 0.09\%$. Using this value, together with an estimate for $\tan^4\theta_c$ of 2.56×10^{-3}, one can deduce the ratio: $\Gamma_{PI}/\Gamma_{SP} = 0.38$.

In the second step, we can use the measured ratio of D^+ to D^0 lifetimes to relate the W exchange contribution to a standard spectator rate, according to

$$\frac{\tau_{D^+}}{\tau_{D^0}} = \frac{\Gamma_{SP} + \Gamma_{WX} + \Gamma_{SL}}{\Gamma_{PI} + \Gamma_{SL}}, \tag{2}$$

where Γ_{SL} represents the rate due to semileptonic charm decay and Γ_{WX} represents any additional contributions having to do with W exchange diagrams (including interference between spectator and W exchange amplitudes). Using the previous result for Γ_{PI}/Γ_{SP} and a D^0 semileptonic branching fraction of 13.4% (muonic and electronic combined), one can extract $\Gamma_{WX}/\Gamma_{SP} = 0.26$.

Finally, to estimate the effects of the weak annihilation diagram, one can use the newest data to compare the D_s lifetime (where weak annihilation is not Cabibbo suppressed) to the D^0 lifetime [7]:

$$\frac{\tau_{D_s}}{\tau_{D^0}} = 1.05 \times \frac{\Gamma_{SP} + \Gamma_{WX} + \Gamma_{SL}}{\Gamma_{SP} + \Gamma_{WA} + \Gamma_{SL}}, \tag{3}$$

from which one can derive $\Gamma_{WA}/\Gamma_{SP} = 0.07$.

Needless to say, these results are only meant to be illustrative of the technique for isolating the various decay contributions, and cannot be taken too seriously by themselves. In practice, one must be attentive of the many uncertainties that feed into the calculations. In some cases, the results are quite sensitive to the input parameters. For example, a variation of $\pm 10\%$ in the semileptonic branching fraction

alone (consistent with measured errors) leads to a range of answers: Γ_{WX}/Γ_{SP}=0.22 to 0.31 and Γ_{WA}/Γ_{SP}=0.04 to 0.11. In general, the lesson one should take away is that all of these contributions can be quite significant and that the current data on charm lifetimes should provide the basis for better understanding in charm decays in the near future.

2.2 Bottom lifetimes

The current data on bottom decays are not far behind the measurements of charm decays. Figure 3 shows the most recent results on bottom lifetimes as reported by the B Lifetime Working Group [8]. Of note is the recent SLD measurement [9] of τ_{B^+}/τ_{B^0}, which is the most precise to date. New measurements of B^+ and B^0 lifetimes are also available from ALEPH [10] and OPAL [11]. Not shown in the diagram is the CDF measurement [12] of the B_c lifetime $\tau_{B_c} = 0.46^{+0.18}_{-0.16} \pm 0.03$ ps.

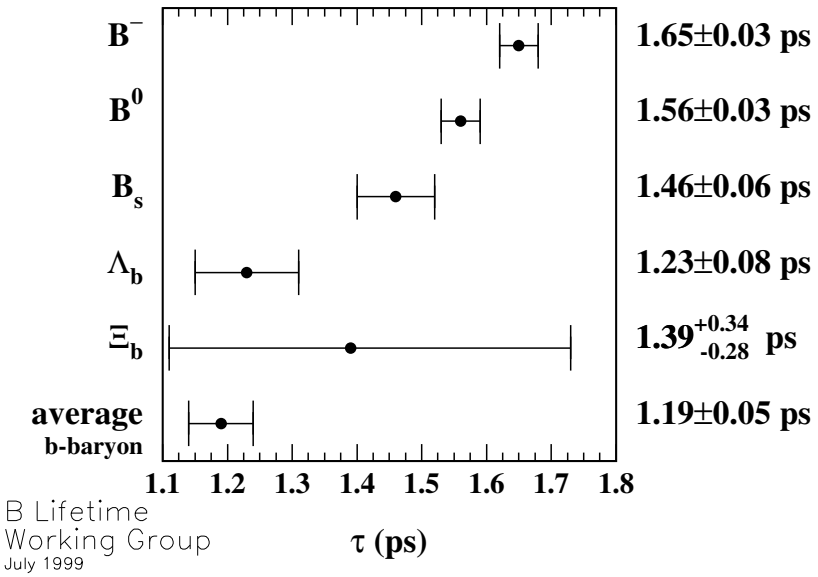

Figure 3: A summary of lifetimes for weakly decaying bottom particles.

The status of the predictions for bottom particle lifetimes is in somewhat better shape than for the charm system. Estimates are usually based on the operator product expansion [13]:

$$\Gamma \approx \frac{G_F^2 m_Q^5}{129\pi^3}(A_1 + \frac{A_2}{m_Q^2} + \frac{A_3}{m_Q^3} + O(\frac{1}{m_Q^4})), \quad (4)$$

which calculates corrections in powers of one over the heavy quark mass. The A_1 term represents the spectator processes, A_2 parameterizes some differences between

the baryons and mesons, and the A_3 term includes W exchange, weak annihilation, and Pauli interference effects. In charm decays, the lighter charm quark mass makes questionable the use of this expansion, but in B decays the correction terms are about 10% of what they are in the charm sector, and this provides a plausible framework for calculation. Figure 4 shows a comparison of experimental measurements and theoretical predictions for several ratios of bottom lifetimes. The shaded area shows the predictions [14]. For the mesons, there is good agreement between theory and experiment, and the measured ratios are close to unity, as expected if the decays are dominated by spectator contributions. For the baryons, the observer might be inclined to wonder at the discrepancy between theory and experiment. It should be noted however, that there are other predictions for bottom lifetimes [15] that are more conservative and include the range of current measurement. This remains a point of controversy.

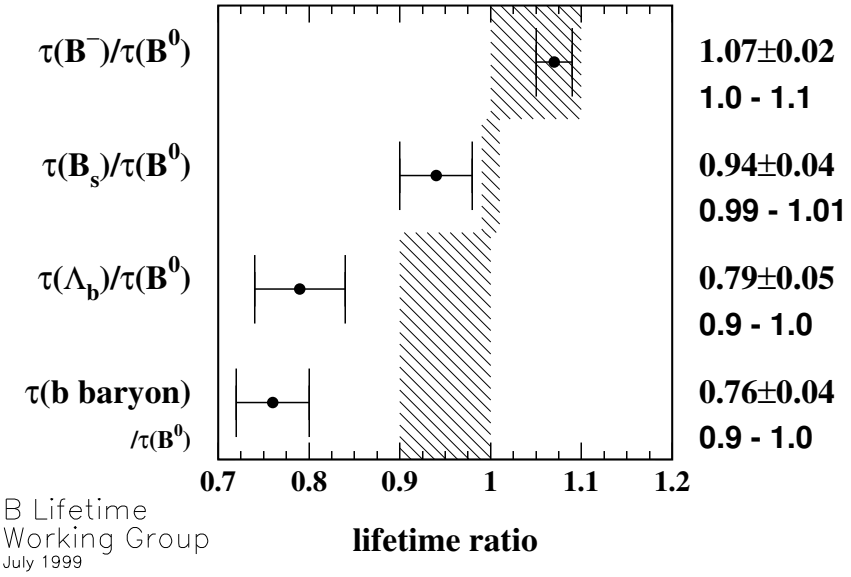

Figure 4: Measured bottom lifetime ratios compared to predictions (shaded) [14].

The next few years will see important new measurements in this sector. Some of the most interesting should come from Run II at the Tevatron. These will provide more precise measurements of the B_s and baryon lifetimes that are needed to reach a general understanding of bottom decays.

3 Meson mixing

Before launching into the latest results on neutral meson mixing, it is useful to begin with a review of the properties of the different systems. Figure 5 shows schematic mass plots for all four neutral systems that are subject to weak flavor mixing [16]. In each case, the scale is artfully chosen to emphasize the mass and width differences between the physical eigenstates. Figure 5a shows the neutral kaon system, with the broad peak of the K_s and, at essentially the same mass, the narrow spike of the K_L, which has a decay width 580 times smaller. Figure 5b shows the charm D^0 system. Although only one curve appears visible, both states of the neutral D have been plotted. The Standard Model predicts an immeasurably small difference in width and mass for the two charm D mesons. Figure 5c depicts the B_d mesons, with essentially the same widths and a small but noticeable difference in mass. Finally, Fig. 5d provides an educated guess for the B_s system. There is expected to be a small difference in width between the two mesons (20% difference in the plot) and a substantial difference in mass. Interestingly, these four systems appear to cover the range of possibilities for mixing.

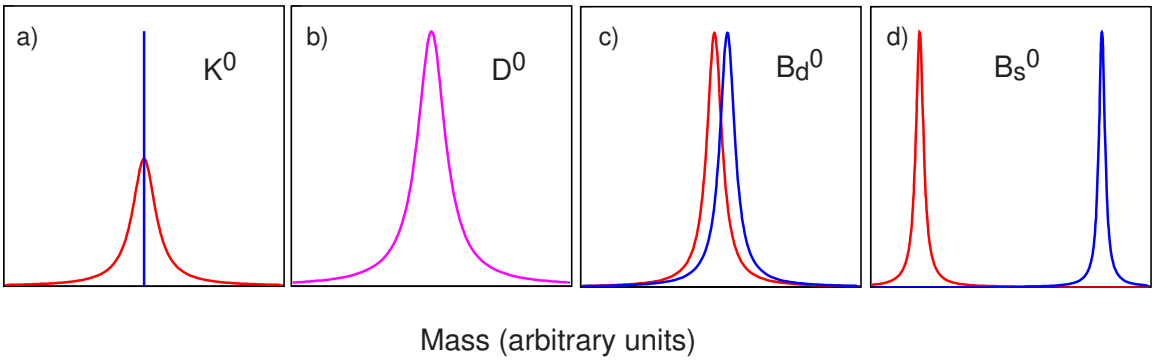

Figure 5: A schematic overview of neutral meson systems subject to flavor mixing.

In order to identify the motivation for studies in meson mixing, it is necessary to understand the source of some of the differences in Fig. 5. Often, the degree of mixing of a neutral meson system is parameterised by

$$r_{mix} \equiv \frac{\Gamma(M \to \overline{M} \to f)}{\Gamma(\overline{M} \to f)}, \tag{5}$$

which describes the rate for a particle to mix and then decay to a particular final state, relative to the rate for the particle to decay to that final state without mixing. In order to calculate the probability of mixing, one usually begins by calculating the amplitudes of flavor-changing box diagrams such as the ones shown in Fig. 6. On

the left is a mixing diagram for the D^0 system. Many such box diagrams contribute with different intermediate quark propagators. In the D system, the intermediate propagators are all down-type quarks. In the B system, the intermediate propagators are all up-type quarks. Calculation of these diagrams shows that the amplitude is proportional to the mass-squared of the intermediate quark. Mixing in the B system is therefore dominated by diagrams with heavy internal top quarks, and consequently the mixing rate is large in this system ($r_{mix} \approx 1$). In D mixing, one would expect that diagrams with the heavy bottom quarks would dominate, but these are strongly suppressed by CKM couplings, and it is actually diagrams with internal strange quarks that dominate [17]. Because the strange quark mass is so much smaller than the top quark mass, this contribution to D mixing is correspondingly smaller than the top quark contribution to B mixing. Moreover, in the charm system it is necessary to feed the heavy charm quark 4-momentum through the light strange quark internal propagators, pulling them off shell in the process and contributing another suppression factor of the form m_s^2/m_c^2. When all is said and done, mixing from SM box contributions to the D system are expected to be extremely small, leading to $r_{mix} \approx 10^{-10}$. Other processes may contribute from on-shell intermediate states [18], nearby resonances [19] or from penguin diagrams [20], but these too are predicted to be very small. Standard Model mixing in the D system is therefore expected to be immeasurable by any current experiment.

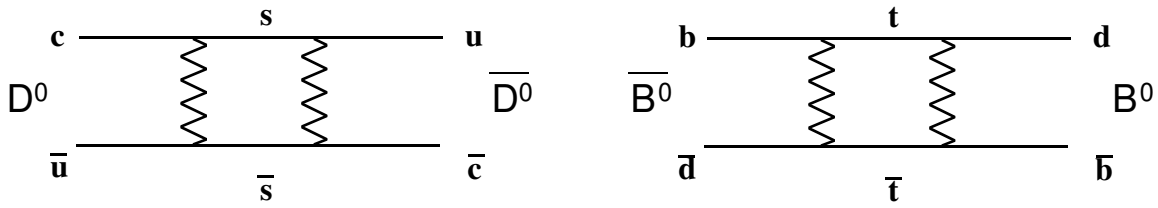

Figure 6: Representative box diagrams that mediate mixing of charm mesons (left) and bottom mesons (right).

The profound difference between mixing in the bottom system and mixing in the charm system is what drives the experimental approach to these systems. In the B system, where mixing from the Standard Model is large, mixing measurements are used to study CKM couplings (most notably V_{td}). In the D system, where SM contributions are small, searches for mixing are used to explore possible contributions from new physics.

3.1 D mixing

The traditional method of observing mixing involves identifying the flavor of the meson both at production and at decay. In this way, it is possible to determine if the meson has mixed during the interim. In the charm system, the most popular means of tagging the produced D is to reconstruct $D^{*+}(D^{*-})$ decays to $\pi^+D^0(\pi^-\overline{D^0})$. In this case, the charge of the pion tells whether the initial D meson is a D^0 or a $\overline{D^0}$. The decay mode of the D can subsequently be used to determine the flavor of the D at decay. As an example, the left diagram in Fig. 7 shows how a D^0 can mix via a box diagram into a $\overline{D^0}$, which then decays via a spectator process to $K^+\pi^-$ or $K^+l^-\overline{\nu}$. Experimentally, if the sign of the reconstructed kaon is the same as the sign of the pion from the D^* decay, then the event is termed a "wrong-sign" event, and is a candidate for D mixing.

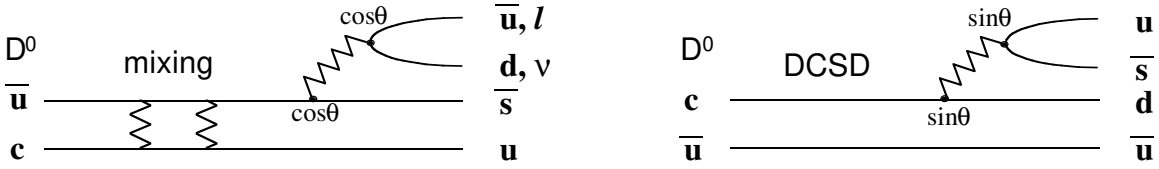

Figure 7: Two diagrams for "wrong-sign" decays of D mesons.

Unfortunately, for hadronic final states, there are two means for producing wrong-sign events. The first involves mixing, as in the left plot in Fig. 7. The second is doubly Cabibbo-suppressed decay, as in the right plot of Fig. 7. Although the DCS rate is expected to be only about 1% of the Cabibbo-favored decay rate, it is an enormous background when compared to the extremely small mixing signal expected. Therefore, the wrong-sign rate for hadronic final states is a combination of three terms: mixing, DCS decay, and interference between the two. Equation (6) shows the time evolution of hadronic wrong-sign decays in the limit of small mixing [21]:

$$\Gamma(D^0 \to K^+\pi^-) \propto e^{-\Gamma t}[4|\lambda|^2 + (\Delta M^2 + \frac{\Delta\Gamma^2}{4})t^2 + (2Re\lambda\Delta\Gamma + 4Im\lambda\Delta M)t], \qquad (6)$$

where λ quantifies the relative strength of DCS and CF amplitudes. The first term, proportional to $e^{-\Gamma t}$, represents the pure DCS decay rate. The second term, proportional to $t^2e^{-\Gamma t}$ represents mixing, which can have contributions from both mass and width differences of the eigenstates. The third term, proportional to $te^{-\Gamma t}$, represents the interference between mixing and DCS amplitudes. In contrast, wrong-sign semileptonic final states are not produced by DCS decays, and the time evolution of those states is simply:

$$\Gamma(D^0 \to K^+l^-\nu) \propto e^{-\Gamma t}(\Delta M^2 + \frac{\Delta\Gamma^2}{4})t^2 \ . \qquad (7)$$

This mode is obviously cleaner theoretically, but more challenging experimentally because of the missing neutrino.

To set the scale for the latest measurements, it is useful to review some previous results. One of the most recent (and least ambiguous) limits on mixing comes from a study at the FNAL E791 experiment [22], which examines semileptonic final states. In that study, the 90% C.L. limit on mixing is $r_{mix} < 0.50\%$, a value that is typical of current measurements. There is also an older CLEO measurement [23] that gives a wrong-sign signal of $r_{ws} = 0.77 \pm 0.25 \pm 0.25\%$. However, because that result did not discriminate between DCS and mixing (there was no vertex chamber for measuring decay lengths in the old detector), it is popularly attributed to DCS decays.

This summer, a new CLEO study [24] that examines $D^* \to D^0\pi \to (K\pi)\pi$ decays shows a dramatic improvement in sensitivity over the older results. This improvement is driven primarily by two effects: excellent mass resolution, which reduces non-D^* backgrounds, and high efficiency at short decay times, which helps to distinguish between DCS decays and mixing. Figure 8 shows plots of the kinetic energy of the $D^0\pi$ system, which should peak at 6 MeV for decays from the D^*. About 16000 right-sign signal events are apparent, with a mass resolution of 190 keV. This impressive resolution is due in part to a new trick being used by CLEO analysts. The slow pion from the D^* decay is required to come from the beam ribbon [25], providing an extra vertex constraint that is an effective aid to improving the momentum resolution.

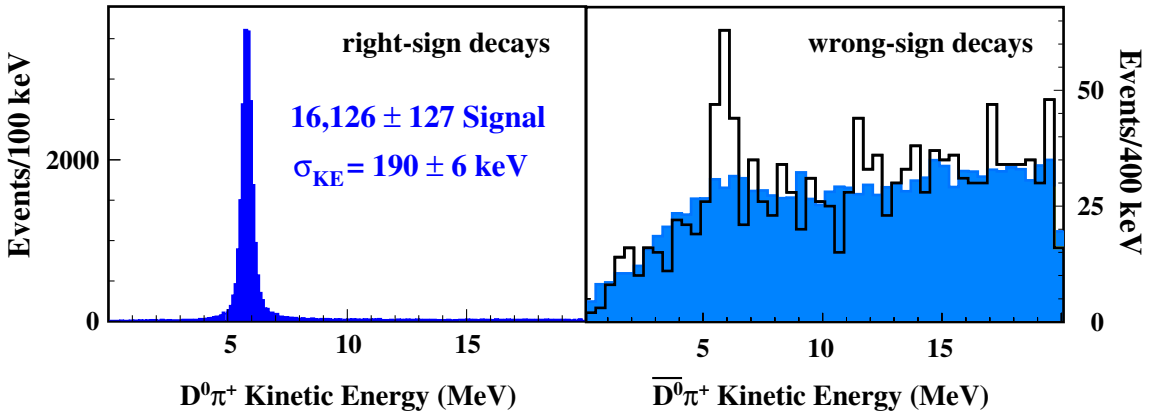

Figure 8: CLEO kinetic energy distribution of right-sign $D^{*+} \to D^0\pi^+$ and c.c. decays (left) and wrong-sign $D^{*+} \to \overline{D^0}\pi^+$ and c.c. decays (right). In the wrong-sign plot, the shaded area shows the expected background level.

The right side of the figure shows the CLEO $D\pi$ kinetic energy distribution for the wrong-sign decays, with about 60 events in the signal peak. A little more than half of the background comes from D^0 to $K\pi$ decays combined with a random pion to give a wrong-sign D^* candidate decay. Smaller background contributions come

from other charm decays and uds events. From these results, CLEO calculates a wrong-sign ratio of $r_{ws} = 0.34 \pm 0.07 \pm 0.06\%$.

To disentangle DCS decays from the mixing contribution, the decay time distribution is fit to the three terms given in Eq. (6). The results are expressed in terms of the parameters x' and y', which are related to the mass and width differences (ΔM and $\Delta\Gamma$) of the physical eigenstates, and the relative phase between DCS and CF decay amplitudes (δ):

$$\begin{aligned} x' &= \frac{\Delta M}{\Gamma}\cos\delta + \frac{\Delta\Gamma}{2\Gamma}\sin\delta \\ y' &= \frac{\Delta\Gamma}{2\Gamma}\cos\delta - \frac{\Delta M}{\Gamma}\sin\delta. \end{aligned} \tag{8}$$

The CLEO 95% C.L. limits are reported as $|x'| < 3.2\%$ and $-5.9\% < y' < 0.3\%$. Assuming that the phase angle δ is approximately zero [26], one can relate these limits to 95% C.L. limits on r_{mix} due to non-zero $\Delta\Gamma$ ($r_{mix} < 0.17\%$ [27]) and non-zero ΔM ($r_{mix} < 0.05\%$).

The reader may note that the r_{mix} limit from the constraint on x' is an order of magnitude more restrictive than previous measurements. The limit from y' is not as restrictive only because the central value for y' is about 1.8 standard deviations away from zero. Although this discrepancy is not terribly significant, it is interesting in its own right. Recently, a direct search by E791 [28] for non-zero $\Delta\Gamma$ has also been performed by looking for a difference in lifetimes for decays to different final states, yielding a sensitivity to $\Delta\Gamma$ comparable to the new CLEO limit. Future work along the same lines can be expected from several experiments.

This subject will be pursued vigorously in the next few years. The FOCUS experiment at FNAL has already shown [29] preliminary results on the decay D^* to D^0 to $K\mu\nu$. From this mode alone, FOCUS expects to be able to set a limit on r_{mix} of about $r_{mix} < 0.12\%$ if there is no indication of mixing. In the near future, B factories will also contribute significantly to these studies. A design luminosity year at BaBar will produce about 10^7 $D^* \to D^0\pi$ decays, which should also lead to some interesting results.

3.2 B mixing

As was suggested earlier, the implied purpose to studying B mixing is to explore CKM parameters, V_{td} in particular. This is easily illustrated with Fig. 9, which shows the triangle corresponding to the CKM unitarity condition $V_{ud}V_{ub}^* + V_{cd}V_{cb}^* + V_{td}V_{tb}^* = 0$. The apex of the triangle is constrained by measurements of V_{ub}/V_{cb} from semileptonic B decays, measurements of CP violation in the kaon system, measurements of ΔM_d from B mixing, and the lower limit on ΔM_s from B_s mixing. The length of the upper right side of the triangle is given by $V_{td}V_{tb}^*/V_{cd}V_{cb}^*$. Because V_{tb} is close to unity,

V_{cd} is well-measured from charm decays, and V_{cb} is approximately $-\sin\theta_c$ in the SM; V_{td} remains the limiting factor in determining the length of that side of the triangle. A precise measure of that side of the triangle would provide excellent complementary information to the angle measurements expected from B factory measurements. Checking consistency in the set of measurements that over-constrain the triangle is of great interest in the search for new physics. In particular, new measurements of V_{td} and $\sin 2\beta$ could constrain the apex of the triangle independently of other data.

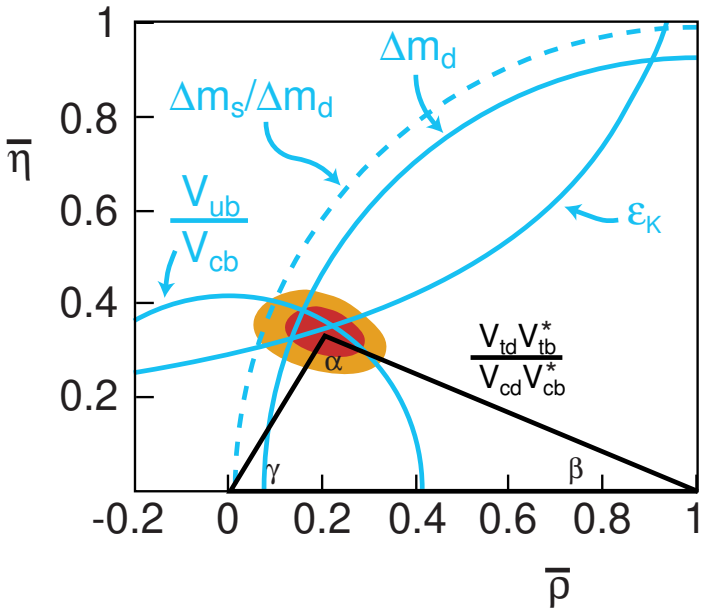

Figure 9: A summary of constraints on the unitarity triangle. Measured central values of ϵ_K, V_{ub}/V_{cb}, and ΔM_d are shown as solid lines without their uncertainties. The 95% C.L. lower limit on ΔM_s is shown as the dashed line. Likelihood contours for the apex of the triangle come from Parodi *et al.* [30].

Equation (9) [31] shows the relationship between the mass difference ΔM_d measured from B_d mixing and the CKM parameter V_{td}. Although the measurement of ΔM_d is now quite good (a total of 26 measurements have been made from LEP, SLD, and CDF [32]), the theoretical uncertainties on the many coefficients in Eq. (9) lead to roughly a 20% uncertainty in V_{td}. However, simultaneous measurements of B_d and B_s mixing can give much better precision on V_{td} through the ratio of mass differences shown in Eq. (10) [33]. In this case, many uncertainties cancel and there remains about a 5% theoretical uncertainty on the extraction of V_{td}.

$$\Delta M_d = \frac{G_F^2}{6\pi^2} m_{B_d} f_{B_d}^2 B_{B_d} \eta_{QCD} F(m_t^2) |V_{td} V_{tb}^*|^2 \qquad (9)$$

$$\frac{\Delta M_s}{\Delta M_d} = \frac{m_{B_s} f_{B_s}^2 B_{B_s}}{m_{B_d} f_{B_d}^2 B_{B_d}} \left|\frac{V_{ts}}{V_{td}}\right|^2 = (1.15 \pm 0.05)^2 \left|\frac{V_{ts}}{V_{td}}\right|^2 \quad (10)$$

To date, ΔM_s has not been measured. Evidence of B_s mixing is clear, but only lower limits on ΔM_s have been determined. Nonetheless, constraints on the unitarity triangle from other measurements suggest that it may be just beyond the current measured limits. Assuming the SM, the contours in Fig. 9 show the present estimate of the apex of the unitarity triangle. The central measured value of ΔM_d suggests the apex should lie on the solid quarter circle centered at $(\overline{\rho}, \overline{\eta}) = (1, 0)$. The limit on ΔM_s ($\Delta M_s > 12.4$ ps^{-1} is used in the figure) corresponds to the dashed quarter circle just outside the ΔM_d curve. Higher limits on ΔM_s push the circle to smaller radius, further constraining the apex of the triangle.

Once again, the identification of mixed events involves tagging the flavor of the meson both at production and at decay, and measuring the time evolution of mixing. The mixing frequency determines ΔM. Several techniques have been utilized for B_s decays. The initial state can be tagged by examining the charge of leptons or kaons in the opposite hemisphere, by examining an associated kaon in the same hemisphere, by calculating a weighted jet charge for either jet, or by using the jet angles in the case of polarized beams. The decaying meson can be tagged by using charged leptons in the final state, by using partially or fully reconstructed D mesons, or by reconstructing two vertices in the decay hemisphere (associated with bottom and charm decay).

The four keys to a precise measure of ΔM_s are excellent proper time resolution, high purity of the B_s decay sample (the worst backgrounds tend to come from other B decays), accurate tagging of the initial and final state mesons, and as always, high statistics. In order to illustrate the challenge to experimentalists, Fig. 10 shows an idealized experiment with infinite statistics and no background for $\Delta M_s = 10$ ps^{-1}. Even in this case, the measurement is not easy. The vertical axis measures the fraction of events identified as mixed, as a function of the proper decay time of the B_s. In a perfect experiment, this curve should start at zero and oscillate between zero and one. The oscillation never makes it all the way to zero or all the way to one because the mistag rate (25% in the figure) dilutes the measurement. This effect is exacerbated by smearing due to decay length resolution (200 μm in the figure). At higher values of proper decay time, the amplitude of the oscillation degrades because of increased uncertainty on the decay time due to the boost resolution (10% assumed in the figure).

Figure 11 shows the combined results on ΔM_s from LEP and CDF. In order to understand this plot, it is necessary to recognize that the probability for mixing is proportional to $1-\cos \Delta M_s t$, where t is the B_s decay time. The figure shows the results of fits for many different values of ΔM_s to oscillation data from many experiments. For each point, the data are fit to a function proportional to $1 - A \cos \Delta M_s t$, where the oscillation amplitude A is a fit parameter. If mixing occurs at that particular value of ΔM_s, then the fitted value of A should be unity. At other values of ΔM_s,

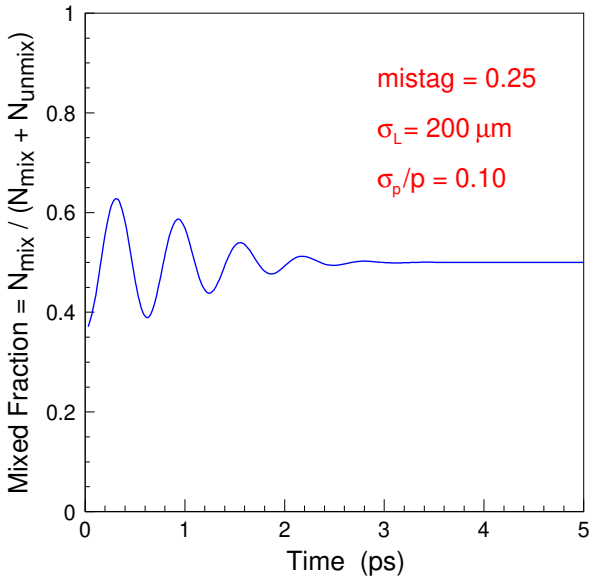

Figure 10: An idealized measurement for B_s mixing using an infinite data sample of pure B_s decays, with $\Delta M_s = 10$ ps^{-1}.

the fitted value of A should be close to zero, consistent with no oscillation. In short, the plot can be thought of as a Fourier analysis of oscillation data, with the vertical axis showing the amplitude A as a function of frequency. The limit on ΔM_s from this plot alone is $\Delta M_s > 13.2$ ps^{-1} at 95% C.L.

Figure 12 is an analogous plot for new data from SLD [34]. These results show dramatic improvement since Moriond 99, driven primarily by new tracking and substantial improvements in decay length resolution. Three separate analyses are employed, corresponding to reconstructed final states of a charm vertex plus lepton, a high-momentum lepton, or a pair of vertices displaced from the primary vertex. Two analyses not shown, but expected in the summer of 2000, search for B_s decays using final states that include an exclusively reconstructed D_s decay, or a lepton and charged kaon. Once again, the plot shows the fitted value of the oscillation amplitude A as a function of ΔM_s. At low values of ΔM_s the uncertainty in A is about a factor of two larger than the results from combined CDF and LEP data. However, at high values of ΔM_s, the uncertainties are comparable, so that these data make a significant contribution to the world average.

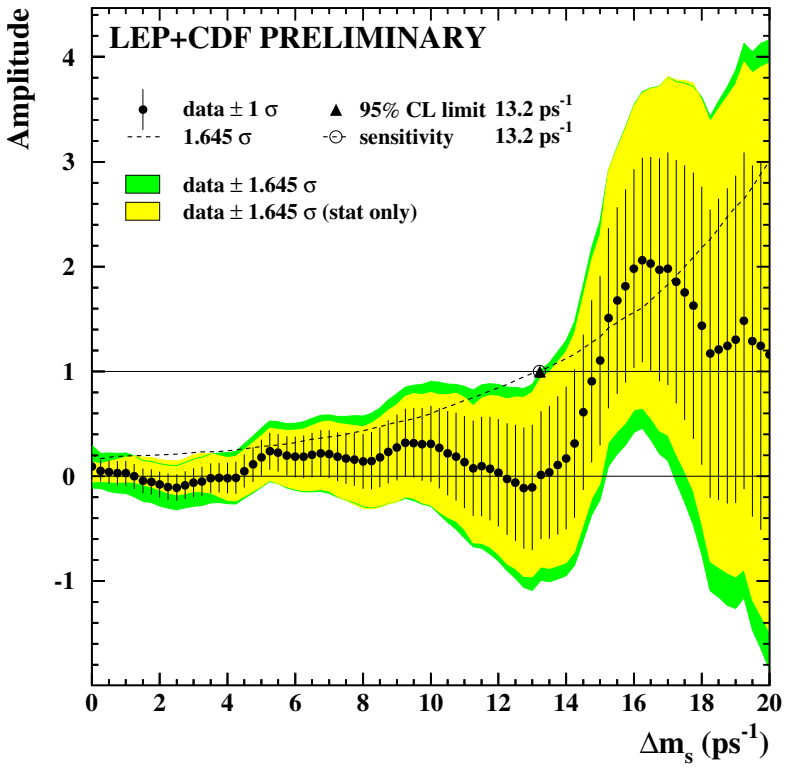

Figure 11: Fitted amplitude for mixing versus the B_s mass difference. LEP and CDF data only.

Figure 13 shows the combined data from all experiments, updated as of December 1999 [32]. A total of 11 analyses contribute. The 95% C.L. lower limit on ΔM_s from these data is $\Delta M_s > 14.3$ ps^{-1}, up from 12.4 ps^{-1} reported at EPS 99 (Tampere). The new higher limit on ΔM_s provides further constraint on the unitarity triangle of Fig. 9. The dashed circle from the ΔM_s limit now moves just inside the curve that represents the central value of ΔM_d. This change clips off a significant fraction of the previously allowed area for the apex of the triangle.

In the next few years, further work in this area should prove very interesting. Figure 14 gives an idea of what we should expect from future studies of B_s mixing. The vertical scale of the plot is called "significance" and is the inverse uncertainty in the amplitude parameter A of Figs. 11-13. It can therefore be interpreted as the analyzing power for discriminating between $A = 0$ and $A = 1$. The squares map the significance as a function of ΔM_s from the combination of all the LEP experiments. The circles plot the significance from the SLD data set when all five analyses are included. Both curves cross the 95% C.L. limit at about ΔM_s=13 ps^{-1}.

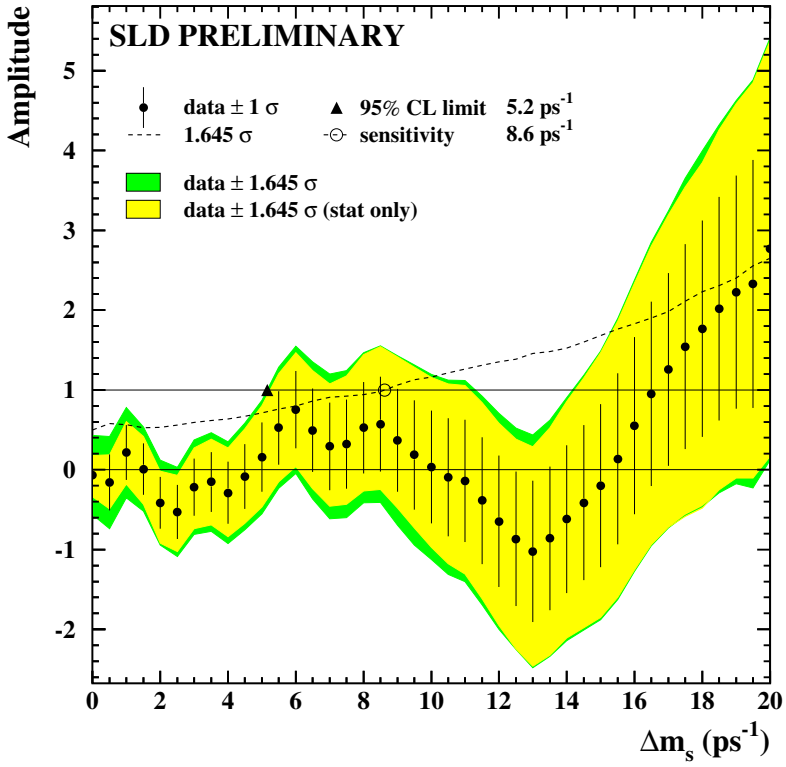

Figure 12: Fitted amplitude for mixing versus the B_s mass difference. SLD results only.

The comparison of these two curves is particularly interesting in two respects. First of all, it is surprising that they appear on the same graph when one considers that the LEP data sample represents 40 times more luminosity than the SLD data sample. Secondly, the shapes of the two curves are significantly different. The SLD curve is dramatically flatter than the LEP curve, and at high values of ΔM_s, the SLD significance even wins out over LEP. The reason for both these features is the very precise vertex resolution of the SLD detector. This allows SLD researchers to do more inclusive style analyses, that are more efficient, in order to compete with the statistics from LEP. It also allows SLD to retain good sensitivity to the very fast oscillation at high values of ΔM_s. The insert in the figure shows the vertex resolution achieved by the ongoing analysis that tags B_s decays via a fully reconstructed D_s decay. The 46 μm resolution for the central Gaussian (60% of the area) is roughly four times better than the resolution achieved in a typical LEP study.

A competitive race will continue between LEP and SLD for the next year or so as each group tries to improve the sensitivity of the measurements. This will be done in the hopes of actually seeing the B_s oscillation, which is predicted by the other

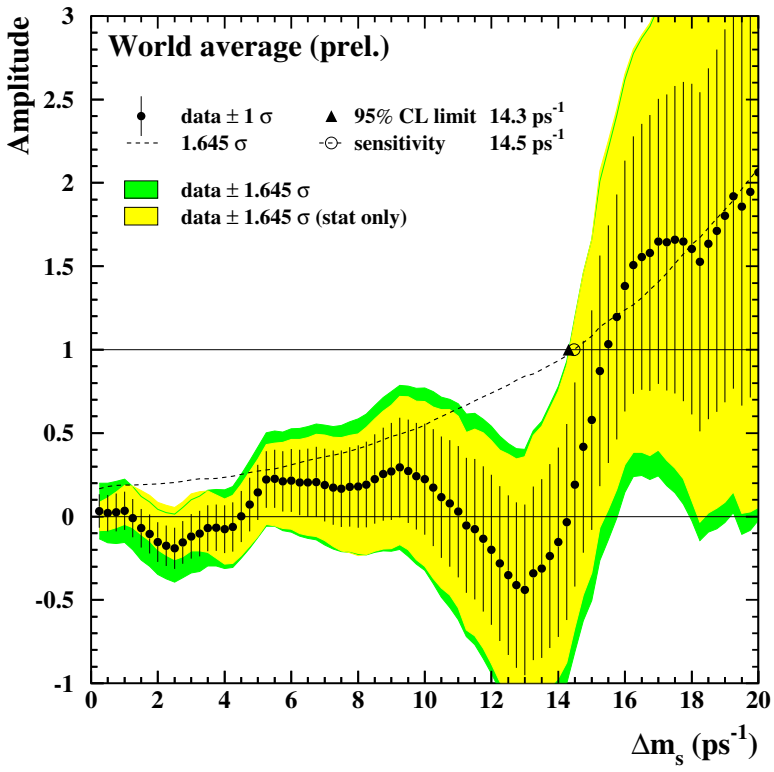

Figure 13: Fitted amplitude for mixing versus the B_s mass difference. Combined world data.

measurements of Fig. 9 as being just beyond the limits of current analysis. However, if the oscillation is not seen at LEP or SLD in the next year, new players will soon dominate the field. The triangles in the upper right corner of Fig. 14 show what to expect from the CDF experiment after Run II. That curve crosses the 95% C.L. line around ΔM_s=50 ps^{-1}. Assuming the Tevatron experiments can trigger efficiently on displaced vertices, those experiments will dominate the B_s oscillation measurements in just a few years. It is especially interesting to note that the future Tevatron data should either confirm the SM estimate of V_{td} or prove that the SM is incorrect because the triangle does not close (see also Michael Peskin's comment at the end of this paper).

4 CP violation

The recent turn-on of two new B factories has focused a lot of attention on the already hot topic of CP violation. This year, there are two items relevant to CPV in the B

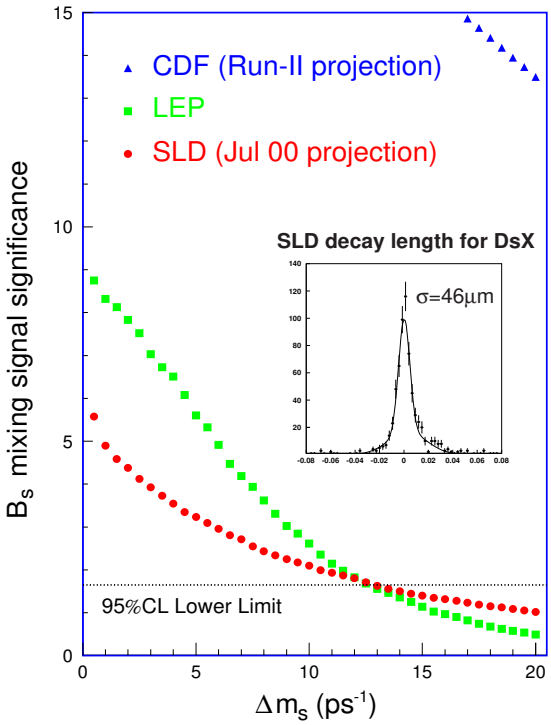

Figure 14: Sensitivity to B_s mixing as a function of the B_s mass difference for three different experiments. The CDF curve (triangles) crosses the 95% C.L. line around $\Delta M_s = 50$ ps^{-1}.

system that are worthy of note. Both of these topics are covered by other speakers at this conference, so the summary here will be brief. The first is an update on searches for CPV in $B^0 \to \psi K_s$ (see also M. Paulini's contribution to these proceedings). The second is a pair of measurements of $\Gamma(B^0 \to \pi^+\pi^-)$ and $\Gamma(B^0 \to K^+\pi^-)$ from CLEO that has implications for future B factory measurements of the mixing angle α (see also R. Poling's contribution to these proceedings).

It is common knowledge that CP violation in a decay rate is due to the interference between two or more amplitudes with different CP-conserving and different CP-violating phases. In particular, if both amplitudes are pure decay amplitudes, then the CP violation is called "direct CPV". In this case, CP violation is constant in time and can be measured via integrated asymmetries. On the other hand, if one of the amplitudes involves mixing then the violation is called "indirect CPV", and the asymmetry evolves in time. In the charm system, where mixing is expected to be negligible, the search for CP violation is generally a search for direct CP violation in integrated asymmetries. In the bottom system, where mixing is large, time dependent asymmetries are used to quantify indirect CP violation.

In the bottom system, measurements of CP asymmetries are used primarily to explore the CKM matrix. From a theorist's view point, final states that are dominated by tree level amplitudes and are CP eigenstates are the cleanest modes for extracting the CKM parameters. Two popular examples of such modes are $B^0 \to \psi K_s$ (which is often considered the golden mode for measuring β) and $B^0 \to \pi^+\pi^-$ (which is often talked about as a method to measure α). Both of these modes have played important roles in recent results.

This year, the CDF experiment has updated a CP asymmetry measurement [35] of $B^0(\overline{B^0})$ decays to ψK_s and a new result from ALEPH [36] for the same final state has also become available. Preliminary indications from CDF were available already last year, but the signal was marginal, and this year researchers have worked hard to squeeze out the last bit of sensitivity from the data. Of the roughly 400 reconstructed ψK_s events in the current CDF data sample, about half of them occur within the acceptance of the vertex detector, where the decay lengths are well-measured. These events are used to measure a time dependent asymmetry in search of CP violation. The other half of the events do not have well-measured decay times and are used in the measure of a time integrated asymmetry. Figure 15 shows the time dependence of the $B^0/\overline{B^0}$ asymmetry with the best fit for an oscillation on the left, and the single data point of the time integrated asymmetry on the right. The two results are combined to get a measure of $\sin 2\beta_{CDF} = 0.79^{+0.41}_{-0.44}$. ALEPH performs a similar time-dependent asymmetry measurement on 23 well-reconstructed decays to get $\sin 2\beta_{ALEPH} = 0.93^{+0.64+0.36}_{-0.88-0.24}$. Together, the two experiments constrain $\sin 2\beta$ to be greater than zero with 98.5% probability. Although this result does not provide a very meaningful test of the previous constraints on the unitarity triangle, it does provide an indication of CPV and some reassurance that this measurement will be a good target for B factory studies in the near future.

The other interesting results this year of relevance to CPV are new measurements [37] from the CLEO collaboration for the branching fractions of $B^0 \to \pi^+\pi^-$ and $B^0, B^+ \to K\pi$. Because the $K\pi$ final states are believed to be dominated by penguin diagrams, these decays offer a measure of the importance of penguin contributions. CLEO measurements for $B \to K\pi$ range from 1.2 to 1.9×10^{-5}, slightly larger than $B \to \pi\pi$ branching fractions, which are believed to be dominated by tree diagrams. The relatively large $K\pi$ branching fractions therefore indicate that penguin diagrams play an important role in these decays. In particular, one can use the measured $B^0 \to K^+\pi^-$ and $B^0 \to \pi^+\pi^-$ rates to get a rough estimate of the $\pi^+\pi^-$ penguin amplitude relative to the $\pi^+\pi^-$ tree amplitude. Following the method outlined in the BaBar physics book [38], Section 6.1.2, one comes to:

$$0.25 < \frac{A^{\pi\pi}_{penguin}}{A^{\pi\pi}_{tree}} < 0.57. \qquad (11)$$

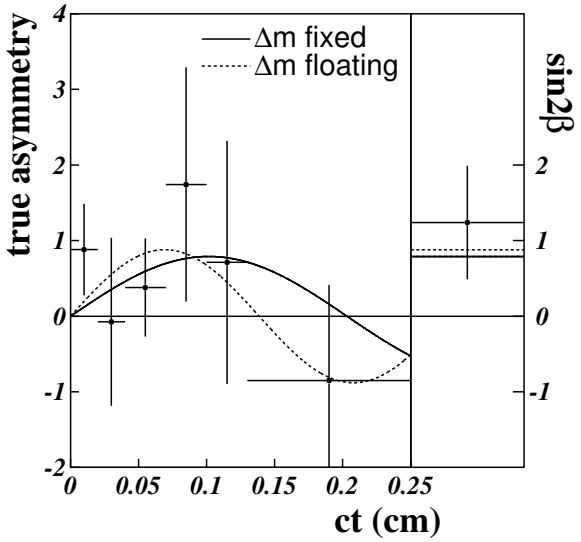

Figure 15: CDF fits to time-dependent (left) and integrated (right) CP asymmetries in $B^0 \to \psi K_s$ decays.

Although the precise numerical result should not be taken too seriously, it does point out that penguin amplitudes are likely to be significant in the $\pi^+\pi^-$ decay mode. Consequently, the study of CPV in the $\pi^+\pi^-$ final state must include interference between tree amplitudes, mixing amplitudes, and penguin amplitudes. This naturally makes the extraction of α much more difficult. As has been pointed out by London and Gronau [39], the $\pi^+\pi^-$ asymmetry can still be used in combination with branching fraction measurements of $B^+ \to \pi^+\pi^0$ and $B^0 \to \pi^0\pi^0$ to measure α, but this is a considerably harder problem, with new ambiguities. The general conclusion is that measurements of α at the B factories will be a challenge.

5 Summary

This paper has examined four topics of recent research in heavy quark decays. In each case, interesting new results are available this year, and these point the way to even better results in the near future. First of all, new measurements of the D_s lifetime provide useful data for improving our understanding in the mechanisms of charm decay. In the near future, precision measurements of charm baryon lifetimes from FNAL fixed target experiments FOCUS and SELEX should help complete that understanding. Secondly, results from a new CLEO search for charm mixing are just released, which improve the sensitivity to charm mixing by about an order of

magnitude. In the next few years, efforts at FOCUS and at the B factories will further the search. Thirdly, attempts to measure the B_s mixing frequency have improved this year, resulting in a higher limit on ΔM_s. Efforts at LEP and SLD will continue for at least another year, with the hope of seeing the oscillation. If it is not found in the next year, Run II data from the Tevatron experiments is expected to extend the reach in ΔM_s by more than a factor of two. In time, this will either confirm the estimates of V_{td}, or it will point to an interesting conflict within the Standard Model. Finally, efforts have begun to measure CP asymmetries in the B system. New results at CDF and ALEPH suggest that $\sin 2\beta$ is within the expected range and should be an easy target for B factory measurements. On the other hand, measurements of α via CP asymmetries of $B^0 \to \pi^+\pi^-$ may prove to be more difficult in light of the new CLEO measurements of the $B^0 \to K\pi$ and $B^0 \to \pi\pi$ branching fractions, which suggest that penguin contributions play an important role in these decay modes.

References

[1] In helicity suppression, spin zero meson decay to a relativistic, back-to-back quark-antiquark pair is suppressed by angular momentum conservation. In color suppression, the final state quarks are required to carry the correct color charge so that the net final state is colorless. For the diagrams of Figs. 1c to 1f, this is an important constraint. For the diagrams of 1a and 1b, correct color matching is already guaranteed by the couplings to the colorless W boson.

[2] C. Caso *et al.*, Eur. Phys. J. **C3**, 1 (1998).

[3] E.M. Aitala *et al.* [Fermilab E791 Collaboration], Phys. Lett. **B445**, 449 (1999) hep-ex/9811016.

[4] G. Bonvicini *et al.* [CLEO Collaboration], Phys. Rev. Lett. **82**, 4586 (1999) hep-ex/9902011.

[5] H.W. Cheung, hep-ex/9912021.

[6] The technique presented here for using charm branching fractions to extract Γ_{PI}, Γ_{WX} and Γ_{WA} was first suggested to me by H. Cheung, Ref. [5].

[7] The factor of 1.05 in Eq. (3) accounts for several small differences in the decay of D_s and D^0 mesons. Purely leptonic decays of $D_s \to l\nu$ lower the D_s lifetime by a few percent, and the presence of Pauli Interference in Cabibbo suppressed D_s decays raises the D_s lifetime by a few percent, as do SU(3) breaking effects. For a complete discussion, see [14].

[8] http://home.cern.ch/~claires/lepblife.html

[9] K. Abe *et al.* [SLD Collaboration], hep-ex/9907051.

[10] G. Calderini [ALEPH Collaboration], CERN-OPEN-99-266.

[11] G. Abbiendi *et al.* [OPAL Collaboration], hep-ex/9901017.

[12] F. Abe *et al.* [CDF Collaboration], Phys. Rev. Lett. **81**, 2432 (1998) hep-ex/9805034; F. Abe *et al.* [CDF Collaboration], Phys. Rev. **D58**, 112004 (1998) hep-ex/9804014.

[13] G. Bellini, I. Bigi and P. J. Dornan, Phys. Rept. **289**, 1 (1997).

[14] I. I. Bigi and N. G. Uraltsev, Z. Phys. **C62**, 623 (1994) hep-ph/9311243.

[15] M. Neubert and C. T. Sachrajda, Nucl. Phys. **B483**, 339 (1997) hep-ph/9603202.

[16] This way of looking at the various flavor mixing systems was first shown to me by Gene Golowich, private communication.

[17] Incidentally, if one keeps all the strange and down quark box diagram contributions to D mixing, the net amplitude is proportional to $(m_s^2 - m_d^2)/M_W^2$. If m_s and m_d were equal, this amplitude would vanish entirely. This is an example of the GIM mechanism at work.

[18] E. Golowich, hep-ph/9706548; F. Buccella, M. Lusignoli and A. Pugliese, Phys. Lett. **B379**, 249 (1996); hep-ph/9601343 J. F. Donoghue, E. Golowich, B. R. Holstein and J. Trampetic, Phys. Rev. **D33**, 179 (1986).

[19] E. Golowich and A. A. Petrov, Phys. Lett. **B427**, 172 (1998) hep-ph/9802291.

[20] A. A. Petrov, Phys. Rev. **D56**, 1685 (1997) hep-ph/9703335.

[21] If the reader is only familiar with mixing in the B system, this formula may be a surprise. In the limit of small mixing, the familiar term $e^{-\Gamma t}\sin^2\Delta m t$ from B mixing is reduced to $e^{-\Gamma t}\Delta m^2 t^2$. In the charm system, new physics may contribute to a width difference as strongly as it does to a mass difference, so the $\Delta\Gamma^2 t^2$ term appears as well.

[22] E. M. Aitala *et al.* [Fermilab E791 Collaboration], Phys. Rev. Lett. **77**, 2384 (1996) hep-ex/9606016.

[23] D. Cinabro *et al.* [CLEO Collaboration], Phys. Rev. Lett. **72**, 1406 (1994).

[24] M. Artuso *et al.* [CLEO Collaboration], hep-ex/9908040.

[25] The beam ribbon constraint is only valid for prompt charm events that originate at the primary vertex. For that purpose, the CLEO analysis requires a minimum D momentum in order to insure that the D did not come from a B decay.

[26] In recent years, fits to charm decay data using certain models have suggested that the phase angle between CF and DCS decay amplitudes is small (for an overview see T. E. Browder and S. Pakvasa, Phys. Lett. **B383**, 475 (1996) [hep-ph/9508362]), but this claim remains controversial.

[27] The limits due to non-zero $\Delta\Gamma$ were calculated from the lower limit of the CLEO constraint on y', $-5.9\% < y'$, with $r_{mix} = y'^2/2$.

[28] E. M. Aitala *et al.* [Fermilab E791 Collaboration], Phys. Rev. Lett. **83**, 32 (1999) hep-ex/9903012.

[29] P. D. Sheldon, hep-ex/9912016.

[30] F. Parodi, P. Roudeau and A. Stocchi, hep-ex/9903063.

[31] G. Altarelli and P. J. Franzini, Z. Phys. **C37**, 271 (1988).

[32] To view the latest summary of measurements of ΔM_d, for B_s mixing, see the B Oscillation Working Group page at http://www.cern.ch/LEPBOSC/.

[33] A. J. Buras, hep-ph/9711217.

[34] K. Abe *et al.* [SLD Collaboration], paper contributued to this symposium.

[35] T. Affolder *et al.* [CDF Collaboration], hep-ex/9909003.

[36] Details on the ALEPH analysis of $B^0 \to \psi K_s$ can be found in the note ALEPH 99-099, available at http://alephwww.cern.ch/ALPUB/oldconf/oldconf_99.html.

[37] Y. Kwon *et al.* [CLEO Collaboration], hep-ex/9908039.

[38] P. F. Harrison and H. R. Quinn [BABAR Collaboration], The BaBar Physics Book, SLAC-R-504 (SLAC, 1999).

[39] M. Gronau and D. London, Phys. Rev. Lett. **65**, 3381 (1990).

Discussion

Michael Peskin (SLAC): There is a comment that is implicit in your discussion of Fig. 9, but it is nice to make it explicit. There is one leg of the unitarity triangle which is determined by V_{ub}. This determination is independent of possible new physics. The long leg on the right is determined by $\Delta m_s/\Delta m_d$. If indeed Δm_s turns out to be of the order of 16 ps^{-1}, then these two measurements would already give an accurate determination of the unitarity triangle in the context of the standard CKM model. On the other hand, this suggestion may turn out to be wrong. But if you made the right hand leg about half that size, it would not be possible to make a triangle. That is, if Δm_s turns out to be greater than about 35 ps^{-1}, the CKM model is wrong or at least incomplete. You noted that the CDF sensitivity goes far beyond this value, up to about 50 ps^{-1}. So when CDF comes into the game, we might determine the CKM triangle within the Standard Model, or we might be able to rule out the Standard Model just on the basis of the Δm_s information.

Jon Thaler (University of Illinois): Ron Poling presented a measurement of γ that is about two σ away from your favored value. Do you have any comments on this discrepancy?

Blaylock: Since I first encountered this question at the conference, I have had time to better understand the assumptions underlying the CLEO analysis [37] that Ron presented. That estimate of γ depends upon a fit to 14 charmless decay modes of the B mesons. By assuming factorization of amplitudes, these decay modes are fit to five parameters. For decay modes that are dominated by spectator diagrams, an argument might be made in favor of factorization since the two ends of the W connect to two separated quark currents (though there is some controversy even about this point). However, most of the modes used in the fit have large penguin contributions, making a factorization argument unreasonable. In my mind it is not surprising that the CLEO fit does not yield the same result for the weak phase γ as other estimates.